Relationships Between the Properties of Fibers and Thermally Bonded Nonwoven Fabrics Made of Polypropylene

ERIK ANDREASSEN,[1,*] OLE JAN MYHRE,[2] EINAR L. HINRICHSEN,[1] MARIANNE D. BRAATHEN,[2] and KRISTIN GRØSTAD[2,†]

[1]Sintef, P.O. Box 124 Blindern, N-0314 Oslo, Norway, and [2]Borealis AS, N-3960 Stathelle, Norway

SYNOPSIS

Typical polypropylene fibers for use in light nonwoven fabrics were produced in a full-scale compact-spinning line. Molecular weight distribution (MWD), extrusion temperature, draw-down ratio, and draw ratio were varied. The fibers were thermally bonded (welded) into nonwoven fabrics, at different bonding temperatures, using a pilot calender line. The tensile properties of the fabrics are influenced by the MWD and the processing conditions of the fibers, and the effects of these fiber parameters increase with increasing bonding temperature. The fabric strength increases with increasing M_w/M_n, decreasing draw ratio, and increasing extrusion temperature, while in all these cases the fiber strength generally follows the opposite trend. Furthermore, the fabric strength, as well as the fiber strength, have a maximum as a function of draw-down ratio. The tensile properties of the fabrics seem to be governed by the bonding properties of the constituent fibers, not the fiber strength per se. Bond characteristics are discussed in terms of skin-core structures. Some details of the macroscopic fracture mechanisms of fabrics were revealed by scanning electron microscopy and the shape of load-elongation curves. © 1995 John Wiley & Sons, Inc.

INTRODUCTION

Woven fabrics are based on yarns. In the production of nonwoven fabrics (nonwovens) the yarn is eliminated. Hence, the production of nonwovens is highly efficient. Spun-bonded fabrics,[1] for instance, which are based on continuous filaments, can be made in a single production line, starting with the melting of the polymer granulates and ending with the bonding of the nonwoven. However, this article deals with conventional nonwovens based on staple fibers.

The thickness of nonwovens may vary from 25 μm to several centimeters, and the areal density from 10 g/m^2 to 1000 g/m^2. A general summary of the properties and applications of nonwovens is given in ref. 1. The individual fibers in a nonwoven are arranged more or less randomly, and the fiber lengths are from a few millimetres long and upwards. For a given areal density, the fabric strength generally increases with a decrease in fiber diameter, and increases up to a limiting value as the fiber length increases.[2] Hence, in order to optimize the strength of a nonwoven the fibers should ideally be long with small diameter. However, too long fibers lead to problems in the carding stage. Regarding the fiber diameter, the trend seems to go towards smaller diameters.

The bonding of fibers can be mechanical, adhesive, or thermal. Mechanical bonding employs the engagement of fibers by frictional forces. A wide range of binder chemicals are used for adhesive bonding. However, adhesive bonding can be obtained without auxilliary chemicals by fiber–fiber welding, usually called thermal bonding.

The equipment used for thermal bonding rely on one or more of the following techniques: (1) direct metal contact, i.e., calendering; (2) air flow through the fabric; and (3) ultrasonic vibrations. This article will focus on the first of these techniques, which is

* To whom correspondence should be addressed.
† Current address: Dyno Industrier AS, Svelleveien, N-2000 Lillestrøm, Norway.

Journal of Applied Polymer Science, Vol. 58, 1633–1645 (1995)
 CCC 0021-8995/95/091633-13

used for nonwovens with areal densities in the range 15–70 g/m^2. The calender rolls can be plain, but one of them usually has an embossing pattern or pins, producing point-bonding. The size, shape, and distribution of the bond spots influence the softness and the tensile properties of the fabrics, as well as the anisotropy.

Thermally bonded nonwovens may consist entirely of polypropylene (PP), but PP can also be found as part of bicomponent fibers (together with polyethylene (PE), polyester, or nylon), and as a binder fiber together with other thermoplastic or nonthermoplastic fibers. PP staple fibers are used at 100% concentration in lightweight nonwovens for hygienic applications. This article will focus on such nonwovens, with typical areal density 20 g/m^2, made of 4–6 cm long staple fibers with linear density 1–3 dtex (the unit dtex is defined as 0.1 g/km).

The literature on thermally bonded nonwovens can be categorized according to its emphasis: Fiber parameters (e.g., morphology and mechanical properties),[2,13] processing conditions (e.g., bonding temperature, pressure, and line speed) and processing equipment (e.g., roll engraving and bending compensation of rolls),[2,14-17] process control (e.g., on-line measurements of fiber orientation and areal density),[18] modeling of the thermobonding process[19-21] and the properties of nonwovens (e.g., tensile properties and permeability),[22-26] lab-scale welding and microscopy studies,[27-32] and special applications. A few relevant articles are summarized below. Some others are referred to when appropriate in the subsequent sections.

A number of thermomechanical processes occur simultaneously in the course of thermal bonding. Warner[21] reviewed some of these mechanisms, and estimated their effects for a typical PP nonwoven. According to Warner, the heat at the center of the bond is probably not only due to the heat conduction from the roll to the fabric. Another source of thermal input is deformation-induced heating, which typically may lead to a temperature raise of 30–35°C. The melting point increases with increasing pressure (the Clapeyron effect). The melting temperature of PP under the bonding pin is typically shifted about 10°C relative to the differential scanning calorimetry (DSC) data obtained at atmospheric pressure. Flow is probably an essential ingredient to the formation of a good bond, and it is generally enhanced by the same changes of parameters that increase the temperature. The (total) interdiffusion of molten polymer molecules is probably not critically important for the bonding.

The fabric strength depends on the degree of interfilament cocrystallization and the conservation of the fiber properties in the fiber core. The crystallization is probably partly deformation-induced. Material that crystallize at the bond perimeter may have been extruded from under the pin during the process, but the resulting structure may be less oriented than in the original fiber. Also, this material may be brittle, due to annealing caused by the elevated temperature. According to Mukhopadhyay,[28] the mechanism of bonding may not be a primary function of the surface energy or even of the crystal morphology, but may rather be principally influenced by the surface topology. Prealignment of polymer chains can occur in surface cracks or channels. It is well known that annealing of filaments prior to thermal bonding results in lower bond strength. This must be due to the perfection of the structure and the smoothing of the surface.

Whitwell et al. studied the effect of cooling rate during thermal bonding.[2,16] The fabric strength had a maximum as a function of cooling rate. This maximum was shifted towards lower cooling rates as the draw ratio of the fiber increased. The occurence of a maximum was explained by the presence of two competing rate-dependent processes. Initially, increasing the cooling rate causes an increase in strength: crystal sizes, voids, and flaws between crystals are reduced, producing stronger bonds and assemblies. Also, at very low cooling rates fractionation will take place: the highest molecular weight species crystallize first, while the lowest molecular weight species are rejected to crystallite boundaries. These short molecules form weak boundary layers, and the macroscopic strength will be low. Concurrently, increasing the cooling rate increases the residual stresses. These stresses originate as adjacent crystals interfere with mutual growth. At low cooling rates, the structure has time to relax, reducing or eliminating the level of residual stresses. At high cooling rates, stresses are frozen in. The structure is weakened by these residual stresses. The reason why the maximum was shifted towards lower cooling rates with increasing draw ratio is perhaps that the level of residual stresses usually increases with increasing draw ratio.

Using a full-scale nonwoven line is an expensive way of evaluating the welding properties of fibers. Mukhopadhyay et al.[27-30] devised a single-bond test that works in the following way: (1) loosely interlinked fiber loops are clamped by two jaws inside a heating chamber. (2) The crosshead is moved in order to produce the required tension in the fibers. (3) The temperature is increased rapidly (rates up to 1000 K/s are available) to a selected value for a

selected period of time and then reduced rapidly to room temperature. (4) One arm of each loop is cut and the specimen is extended until it breaks. The advantage of this method is that it is quick and gives information about a single bond. However, single bonds are not encountered in thermally bonded fabrics, and it is not straightforward to convert testing parameters to actual processing parameters (the bonding time, for instance, is usually 60 s in these tests). Yet, the method may still be relevant for testing welding properties, and for more fundamental studies. For a range of commercial fibers the maximum bond strength measured by this test is correlated with the grading of bonding performance in industrial processing of nonwovens. Also, the effects of bonding time, temperature, and pressure agree qualitatively with full-scale trials.

Wei et al.[12] studied the effects of bonding temperature on a wide range of nonwoven properties, using PP fibers with different diameters and draw ratios. Our study follows the same philosophy as that of Wei et al., but it is extended to include effects of the molecular weight distribution (MWD) and other fiber processing parameters than the draw ratio. However, our study is limited to the tensile properties of the nonwovens. The work reported in this article is a continuation of our earlier studies of the structure and properties of PP fibers.[33-37]

EXPERIMENTAL

Fibers

Fibers with linear density 2.2 dtex were produced in a Rieter-Automatik (RA) compact-spinning line. (Details on compact and conventional spinning lines, and the associated processing parameters, can be found in refs. 34 and 38.) Hence, the diameter of the fibers is roughly 18 μm. This is the standard diameter for fibers in thermally bonded PP nonwovens for hygienic applications. The original experimental design consisted of 16 trials, in which M_w/M_n, extrusion temperature, die diameter (i.e., draw-down ratio) and draw ratio were varied independently in two levels; 3.8/4.6, 240°C/280°C, 0.25/0.40, and 1.2/1.6, respectively. However, the processing window of the spinning stage was narrower than expected, and spinning parameters had to be adjusted in order to achieve stabile processing conditions. Some of the original trials (11–15) required extensive adjustments, and were, hence, omitted.

The modified experimental design is shown in Table I. In accordance with commercial practice for fibers of this kind, a narrow range of draw ratios was selected. In order to have large variations in the draw-down ratio, dies with different diameters were used (all spinnerets had 30,500 orifices). Draw-down ratios, calculated from the final fiber diameter, the draw ratio, and the die diameter are also shown in Table I. The design was supplemented by two "midpoint" trials: A17 and A18. Some of the trials were repeated after some time, in order to check the reproducibility of the spinning line.

The fibers A1–A16 were produced from homopolymers with melt flow index (MI) 16. The narrow MWDs were obtained by peroxide degradation. A17 and A18 were produced from homopolymers with MI = 12 and 25, respectively.

The RA line differs from the Barmag line used in this and earlier studies[33-37] in a number of ways: the dies are shorter and have constant diameter, and there are three stages after the drawing stage: (1) stuffer box crimping;[38] (2) drying/annealing (fibers transported unconstrained on a conveyer belt, ~ 1 min at 80°C); and (3) cutting.

In order to compare RA and Barmag compact-spinning lines, and supplement the incomplete RA matrix (Table I), a series of fibers with "hygiene" parameters was run on a Barmag line. The spinneret had 20,000 orifices with an exit diameter of 0.35 mm. These Barmag fibers were not converted to nonwovens. The following four parameters were varied independently in two levels: M_w/M_n (3.8 and 4.6), extrusion temperature (260° and 280°C), draw ratio (1.2 and 1.6), and fiber diameter (1.8 dtex and 2.5 dtex). Only one spinneret was used in the Barmag trials. Hence, the draw-down ratio was varied in four levels (between 180 and 335) via the extrusion rate and the fiber diameter.

All fibers were characterized by tensile testing, density measurements, differential scanning calorimetry (DSC) and wide-angle x-ray scattering (WAXS) (Laue camera).

Nonwoven Fabrics

The RA staple fiber samples (A1–A18) were carded and bonded into nonwoven fabrics on a Hergeth Hollingsworth nonwoven pilot line. The temperature of the calender rolls was varied. All other nonwoven processing parameters were kept constant. The upper and lower calender rolls were held at the same temperature. Four temperatures were used: 143, 146, 149, and 152°C. A roll temperature of 155°C, which is often used by the industry, was also tried. However, at this temperature it was impossible to run the nonwoven line, because the fibers would adhere

Table I Experimental Design for the Production of Fibers on the RA line

Sample	M_w/M_n [−]	Extrusion Temperature [°C]	Die Diameter [mm]	Draw Ratio[a] [−]	Draw-Down Ratio[b] [−]
A1	4.6	260	0.25	1.6	105
A2	3.8	260	0.25	1.6	105
A3	4.6	240	0.25	1.6	105
A4	3.8	240	0.25	1.6	105
A5	4.6	255	0.4	1.6	268
A6	3.8	255	0.4	1.6	268
A7	4.6	240	0.3	1.6	151
A8	3.8	240	0.3	1.6	151
A9	4.6	260	0.25	1.2	139
A10	3.8	260	0.25	1.2	139
A16	3.8	240	0.3	1.2	201
A17	4.4	270	0.3	1.4	172
A18	4.4	260	0.3	1.4	172

[a] The (solid state) draw ratio is defined as the ratio of line speed to spinning speed.

[b] The (spinning stage) draw-down ratio is defined as the ratio of spinning speed to extrusion speed. These draw-down ratios were not set independently; they were calculated from the other parameters.

to the rolls. All fabrics consisted of a monolayer with areal density 20 g/m^2.

It is known that fiber–fiber friction, fiber–metal friction, the amount of spin finish, and the electrostatic properties of the fibers influence the carding stage prior to bonding. Only small variations in these quantities were observed, with no statistically significant effects on the tensile properties of fabrics.

The nonwoven fabrics are named NAx, where NA1 is based on the fiber A1, etc. If not otherwise stated, the fabrics referred to in subsequent sections were bonded at 152°C.

The tensile properties of these nonwovens were measured both in the machine direction (MD) and in the cross-direction (CD) on samples that were 5 cm wide and 20 cm long (in the testing direction). The samples were tested at a constant crosshead speed of 10 cm/min at room temperature. There was some variation in areal density among the fabrics, but all the tensile measurements were normalized to an areal density of 20 g/m^2. Some of the nonwovens were examined by scanning electron microscopy (SEM), as produced and after being deformed and fractured.

PROPERTIES OF FIBERS

Structure development in the compact-spinning process, and the resulting tensile properties, and melting characteristics of the fibers have been reported earlier.[34,36] However, the draw-down ratios are generally higher for the fibers in the present study. The major differences compared to earlier studies will be pointed out in the subsections below. The same major trends were observed for both RA and Barmag fibers.

Structure, Molecular Orientation, and Density

High spinline stress leads to orientation-induced crystallization and monoclinic (α) structure with bimodal orientation.[34] Due to the high draw-down ratios in this study, all the fibers obtain α-crystalline structures with various degrees of bimodal orientation.

The x-ray diffractograms of narrow MWD fibers have broader peaks, indicating less ordered and/or smaller crystallites. This agrees with earlier findings.[37] A new trend, compared to ref. 34, was observed in this draw-down ratio regime: narrow MWD fibers obtain higher molecular orientation than broad MWD fibers (the narrow MWDs in this study are somewhat broader than those in earlier studies). This can, for instance, be seen for the four broad/narrow MWD pairs with draw ratio 1.6 (fiber A1–A8). (Earlier, we have only observed this trend at high draw ratios (> 3), since narrow MWDs are drawn more effectively in the solid state.[34]) A similar MWD effect on orientation has been reported in studies of high-speed spinning,[39] where the draw-down ratio is high. This MWD effect is also consistent with our earlier results for fibers with low draw ratios and bimodally oriented α-crystalline struc-

ture: the orientation of narrow MWD fibers increases relative to that of broad MWD fibers (i.e., the difference between narrow and broad MWD fibers decreases) as the draw-down ratio increases.

The pairs A1/A9, A2/A10, and A8/A16 only differ with respect to draw ratio and draw-down ratio. As expected, fibers with a high draw ratio have the highest degree of orientation, because the structure development is usually dominated by the draw ratio.

The pairs A1/A3 and A2/A4 only differ with respect to extrusion temperature, while the pairs A3/A7 and A4/A8 only differ with respect to die diameter (i.e., draw-down ratio). The pairs A1/A5 and A2/A6 have different draw-down ratios, but almost the same extrusion temperature. With the Laue (WAXS) method used in this study, there were no discernible differences in the degree of orientation for any of these pairs. However, among the narrow MWD fibers, A6, which has the highest draw-down ratio, has the highest degree of orientation. In contrast to this, the variation in orientation among the broad MWD fibers with the same draw ratio (A1, A3, A5, and A7) is small. The reason for this difference between narrow and broad MWDs could be that the orientation of the latter "saturates"[39,40] at a lower draw-down level. At the highest draw-down ratios, the deformation may be too fast for the longest chains to respond. In narrow MWDs, however, these long chains are absent, and a large fraction of the chains, with shorter relaxation times, may achieve a high degree of orientation, and form a basis for the fiber morphology.

The densities are in the range 0.89–0.90 g/cm^3 (see Table II). Broad MWD fibers generally have somewhat higher density. This could be due to a higher degree of orientation-induced crystallization, because this phenomenon is known to be sensitive to the high-molecular-weight tail of the MWD. Differences in the degree of crystallinity could not be discerned from the Laue (WAXS) films.

Tensile Properties

Values for the tensile modulus, elongation at break, and tenacity at break (i.e., tensile strength) are reported in Table II. As expected from the previous subsection and earlier studies,[34] narrow MWD fibers have higher strength, lower elongation at break, and steeper load–elongation curves between yield and break. The strength also increases with increasing draw-down ratio (cf. the pairs A3/A7 and A4/A8) and draw ratio (A1/A9, A2/A10, and A8/A16).

The measurements of elongation at break and strength are in the ranges 220–370% and 15–23 cN/tex, respectively. The three strongest fibers (A2, A4, and A8), with tensile strength above 20 cN/tex, have a high draw ratio and a narrow MWD. The only other fiber with high draw ratio and narrow MWD (A6) has lower strength than these three. This is not due to the extrusion temperature (compare A6 with A2) or the elongation rate (i.e., throughput, compare A6 and A8). Fiber A6 was produced with the largest die diameter, i.e., the highest draw-down ratio. For a given die, the tensile strength is known to increase with increasing draw-down ratio, just as the degree of orientation. Fiber

Table II Selected Fiber Properties

Sample	Bulk Density [g/cm^3]	Tensile Modulus [cN/tex][a]	Elongation at Break [%]	Tensile Strength [cN/tex][a]	Onset of Melting [°C]
A1	0.893	56	294	16.6	157.2
A2	0.889	73	232	23.3	154.1
A3	0.897	67	248	17.3	157.6
A4	0.891	68	227	21.6	154.7
A5	0.892	67	286	18.4	157.4
A6	0.890	53	225	18.2	155.2
A7	0.891	73	252	18.4	157.5
A8	0.891	71	217	22.6	155.1
A9	0.891	64	369	15.5	158.0
A10	0.896	65	287	18.0	155.8
A16	0.890	53	273	15.5	156.5
A17	0.899	62	354	15.4	157.0
A18	0.893	65	331	14.6	156.8

[a] 1 cN/tex corresponds to about 9 MPa for these fibers.

A6 has higher orientation than A2, A4, and A8, but lower strength. This can be due to structural defects or diameter variations caused by the high draw-down ratio and/or the die design. (As mentioned in the Experimental section, the extrusion temperature and the throughput had to be adjusted in order to stabilize the spinning of this fiber.) According to Yoo,[41] draw resonance occurs above a critical draw-down ratio, as the take-up force starts to decrease, due to decreasing elongational viscosity. Note that fiber A6 has just as low elongation at break as A2, A4, and A8. The same trend, i.e., a maximum in tensile modulus and strength vs. draw-down ratio, can be seen for the broad MWD fibers A1, A3, A5, and A7. The variability (standard deviation and coefficient of variation) of the tensile strength of A5 and A6 is not higher than that of the other fibers.

Melting Behavior

Values for the onset of melting, as measured by DSC, were in the range 154–158°C (see Table II). The onset temperature increases with increasing M_w/M_n, decreasing draw ratio, decreasing extrusion temperature, and increasing draw-down ratio, as reported earlier.[36] The difference in onset temperature between narrow and broad MWD fibers is the most pronounced of these effects.

A shoulder or secondary peak appears on the high temperature side of the main peak in some cases. This secondary peak is more pronounced (compared to the primary peak) for fibers with narrow MWD, high draw ratio, and low draw-down ratio. For some of these fibers (e.g., A2 and A4) the area under the secondary peak is larger than that under the primary peak. The position of the secondary peak, and the temperature at which the last structural element melts, is almost independent of material and processing parameters. The secondary peak may be due to the melting of structures that have been reorganized and/or perfected during the heating scan.[36]

PROPERTIES OF NONWOVEN FABRICS

The tensile properties of the nonwovens are summarized in Tables III and IV. Compared to commercial nonwovens of this kind, the tensile properties are somewhat inferior and the anisotropy is high. However, the absolute values are not so interesting in this study; we will, instead, identify relationships between fiber and nonwoven properties by examining the differences in nonwoven properties.

Table III Tensile Properties of Nonwoven Fabrics Bonded at 152°C

Sample	MD Load at 10% Elongation [N/5cm]	σ_{MD}[a] [N/5cm]	ε_{MD}[b] [%]	σ_{CD}[a] [N/5cm]	ε_{CD}[b] [%]	BI[c] [N/5cm]	AI[d] [−]	R[e] [−]
NA1	13.4	21.6	24	2.9	61	7.8	7.5	0.13
NA2	13.6	17.5	16	2.6	47	6.7	6.8	0.08
NA3	16.1	22.0	18	2.4	41	7.2	9.3	0.13
NA4	13.2	17.1	16	1.7	34	5.5	9.8	0.08
NA5	12.3	14.4	14	1.3	33	4.3	11.5	0.08
NA6	13.3	18.0	17	2.6	55	6.8	7.0	0.10
NA7	16.4	26.1	23	3.9	62	10.1	6.7	0.14
NA8	16.4	23.5	19	2.9	49	8.3	8.0	0.10
NA9	16.0	27.9	34	4.3	72	10.9	6.5	0.18
NA10	14.9	23.3	24	3.6	58	9.1	6.5	0.13
NA16	19.7	34.1	31	4.9	82	12.9	7.0	0.22
NA17	—	30.4	38	3.8	67	10.8	7.9	0.20
NA18	—	24.0	29	4.9	86	10.8	4.9	0.16

[a] The strength of the fabric, defined as the maximum of the load-elongation curve. The unit N/5cm is commonly used for such fabrics; the width of the test samples is 5 cm.

[b] The elongation at which the load-elongation curve has its maximum.

[c] The bondability index (BI) is defined as $\sqrt{\sigma_{MD} \cdot \sigma_{CD}}$.

[d] The anisotropy index (AI) is defined as σ_{MD}/σ_{CD}.

[e] The ratio of MD fabric strength to fiber strength. The nominal stress unit cN/tex, which is used for fibers, corresponds to 10 N/5cm for a fabric with areal density 20 g/m^2.

Table IV Tensile Properties of Nonwoven Fabrics Based on Fiber A16, Bonded at Different Temperatures

Bonding Temperature [°C]	σ_{MD} [N/5cm]	ε_{MD} [%]	σ_{CD} [N/5cm]	ε_{CD} [%]	BI [N/5cm]	AI [−]
143	14.7	9	0.9	20	3.7	16.0
146	20.6	15	1.3	27	5.2	15.7
149	28.8	21	2.6	42	8.6	11.2
152	34.1	31	4.9	82	12.9	7.0

Effects of Calender Roll Temperature on the Tensile Properties

The dominant processing parameter is the temperature of the calender rolls, i.e., the bonding temperature. When running a new fiber grade, this is usually the only parameter that is adjusted; nonwovens are produced at different calender temperatures and subjected to tensile testing.

MD and CD strengths, and the corresponding elongations, usually have a maximum as a function of bonding temperature, at roughly the same temperature.[9] Both the maximum nonwoven strength and the temperature at which it is obtained can be quite different for two different PP fibers. The peak of, for example, MD strength vs. bonding temperature, should not be too sharp, in order to ensure a stabile process.

A possible explanation for the coincident maximums of the fabric strength and the corresponding elongation is that when the bonds are optimal, the fabric response is closest to the fiber response. [The strength and elongation at maximum load of a nonwoven are, of course, lower than those of the constituent fibers (in comparable units); we will return to this topic in the next section.] As the bond quality decreases, above and below the optimum bonding temperature, the bonds' responsibility for fracture increases. A lower bonding temperature leads to a lower bond strength, but too high bonding temperatures are detrimental to the fiber strength.

In our study, the MD and CD strengths increase monotonously, as shown in Table IV. However, the high-temperature window could not be probed, as reported in the Experimental section. The strength and the elongation at maximum load are positively correlated; both increase with the degree of bonding. Wei et al.[12] also reported that the MD breaking elongation increased as a function of bonding temperature for fibers with low draw ratios, but it decreased for fibers with high draw ratios. The latter result does not agree with our observations and the discussion in the preceding paragraph. The data of Wei et al. are not fully compatible with ours: the highest draw ratio was as high as 3 in their study. Furthermore, the fabrics had areal densities of 90–100 g/m^2 and were fused by direct heating in a hot press.

The anisotropy indices (AIs) in Table IV decrease with increasing bonding temperature. This is because the CD strength is more influenced by the bonding than the MD strength: fibers aligned perpendicular to the testing direction will only contribute to the fabric strength if they are bonded. There are more fibers "perpendicular" to the CD direction than to the MD direction. Hence, the degree of anisotropy decreases as the degree of bonding increases.

Effects of Fiber Parameters on the Fabric Properties

The effects of fiber parameters increase as the bonding temperature increases. The difference between the strongest and the weakest fabric, in terms of MD strength, increases by more than a factor 2 as the bonding temperature increases from 143 to 152°C. The corresponding difference in CD strength increases by a factor 5.

Different units are used for the strengths of fibers and fabrics. For fabrics with areal density 20 g/m^2, it is easy to show that the nominal stress unit cN/tex, which is used for single fibers, corresponds to 10 N/5cm. The ratio of MD fabric strength to fiber strength has values in the range 0.1–0.2, and it is positively correlated with the fiber strength (see Table III). As a comparison, Mukhopadhyay et al., in a study of bonds between commercial single fibers (cf. Introduction), observed ratios of bond strength to fiber strength in the range 0.2–0.8.[29]

MWD Effects

If all processing variables are kept constant, fabrics based on broad MWDs have higher strength and

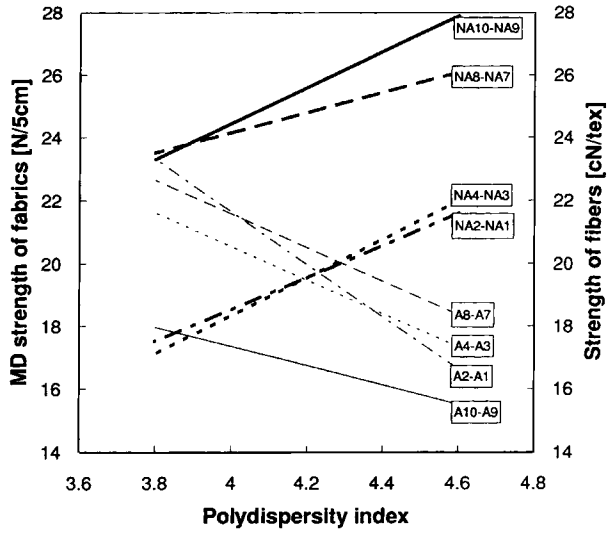

Figure 1 MD strength of nonwovens (thick lines) and strength of the constituent fibers (thin lines) as function of polydispersity index (M_w/M_n). The bonding temperature is 152°C for all the fabrics. As explained in the main text, the unit N/5cm corresponds to 0.1 cN/tex.

elongation at maximum load than fabrics based on narrow MWDs (see Fig. 1). The only exception from this in our study is the pair NA5/NA6. As discussed above, the high draw-down ratio that was used in the spinning of A5 and A6 may have lead to anomalies in the form of structural defects or large diameter variations. Narrow MWD fibers are less prone to spinning instabilities.[41] This may explain why NA6 is stronger than NA5.

The load level prior to maximum load is less correlated with the MWD than the strengths, cf. the MD loads at 10% elongation in Table III.

Tensile strengths of constituent fibers are also shown in Figure 1, and ratios of MD fabric strength to fiber strength are given in Table III. Two of the narrow MWD fabrics (NA2 and NA4) have less than 10% of the fiber strength, while all the other fabrics in Figure 1 have more than 10% of the fiber strength. Note that the strongest fabric in Figure 1, NA9, is based on the weakest fiber.

For all the broad/narrow MWD pairs, except A5/A6, the broad MWD gives the weakest fiber but the strongest fabric. The A5/A6 pair have equal fiber strengths, but the broad MWD gives the weakest fabric, i.e., there is no "inversion" of strengths, going from fiber to fabric, for this pair. This is another indication of the anomalous properties of these two fibers.

Why are fabrics that are made of narrow MWD fibers generally weaker than fabrics made of broad MWD fibers, even though the narrow MWD fibers themselves are stronger? A tentative explanation may be that for a narrow MWD fiber, the bonding process melts and destroys more of the fiber structure. The high-molecular-weight tail of a broad MWD fiber initiates orientation-induced crystallization, which leads to crystalline structures with a high melting point.[36,42] These fibers also have a higher degree of crystallinity. The fibers only feel the temperature in the bonding zone for a fraction of a second, and broad MWD fibers probably preserve more of their structural integrity in the bonding process. Finally, broad MWD fibers have a lower degree of (bulk) molecular orientation. If the orientation is lower at the surface as well, this may facilitate bonding.

Effects of Draw Ratio and Draw-Down Ratio

A trend that has been discussed in the literature[12] is that the fabric strength decreases with increasing fiber draw ratio. Our data also seem to support this, as shown in Figure 2. A possible explanation for this draw ratio effect is that too high molecular orientation at the surface is detrimental for the interfilament cocrystallization taking place during bonding. Fibers with high draw ratios may also be more prone to defects induced by the heat and stress during the bonding process.

The fiber pairs with different draw ratios in Figure 2 also have different draw-down ratios, because the final diameter is the same for all fibers. The draw

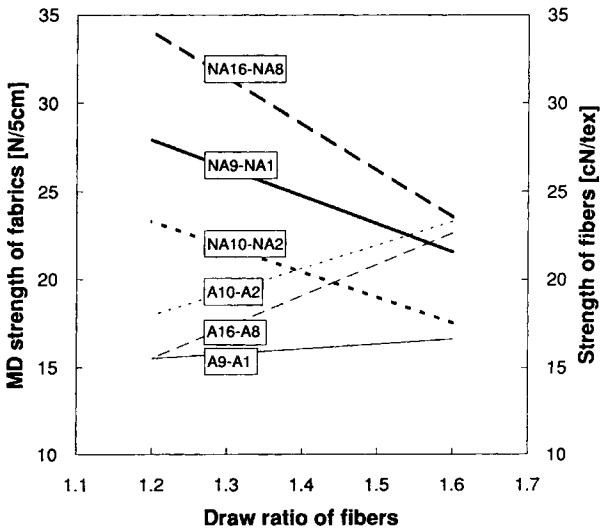

Figure 2 MD strength of nonwovens (thick lines) and strength of the constituent fibers (thin lines) as function of (fiber) draw ratio. The bonding temperature is 152°C for all the fabrics. As explained in the main text, the unit N/5cm corresponds to 0.1 cN/tex.

ratio is considered to be the most important parameter for the fiber properties. This is also the case for the fibers produced in this study, as mentioned above. However, it is not necessarily the case for the nonwoven fabrics. The effects seen in Figure 2 may also be due to different draw-down ratios, i.e., a positive correlation between fabric strength and draw-down ratio. The fabrics in the pairs NA3/NA7 and NA4/NA8 only differ with respect to the draw-down ratio. For the NA4/NA8 pair, the strength difference is just as large as between the pairs in Figure 2. The difference is somewhat smaller for the MD strengths of the pair NA3/NA7. In the cross-direction, both of these pairs have roughly the same strength difference as the pairs in Figure 2.

Because the two pairs that only differ with respect to the draw-down ratio have about the same difference in both MD and CD strength as the pairs in Figure 2, the trends in Figure 2 may be due to a combination of draw-down ratio and draw ratio variations. From this truncated experimental design we cannot say that one parameter is more important than the other, because by far the strongest fabric is made from fiber A16, which has a low draw ratio and a high draw-down ratio (only the deviating fibers A5 and A6 have a higher draw-down ratio, see below). Furthermore, apart from the NA16 fabrics, the strongest fabrics have low/medium draw ratios and medium/high draw-down ratios.

The pairs NA1/NA5 and NA2/NA6 also have low/high draw-down ratios. For the latter pair, a small increase in the tensile strength is observed with an increase in draw-down ratio. For the former pair of fabrics a rather large decrease is observed. However, as discussed earlier, the fibers A5 and A6 have a very high draw-down ratio and probably fall outside the general patterns; at such high draw-down ratios both the fiber strength and the fabric strength decrease with increasing draw-down ratio. These pairs also have slightly different extrusion temperatures. However, we do not believe that this variation in extrusion temperature has any great influence on the fabric properties, because the MD strengths of the fabrics in the pairs NA1/NA3 and NA2/NA4, which differ with respect to extrusion temperature by 20°C, are roughly the same.

There may be several reasons for the effect of the draw-down ratio. An increase in the draw-down ratio will lead to increased molecular orientation and orientation-induced crystallization.[34] The effect of this would again be a better preservation of the fiber (core) at the bonding point, as discussed for the MWD effect. However, WAXS (Laue photography) patterns show larger orientation differences due to the draw ratio (the pairs in Fig. 2) than due to the draw-down ratio alone, and, hence, too high orientation seems to lead to weak bonds. Another and perhaps more important effect of increasing the draw-down ratio could be to increase the degradation of the polymers at the surface of the fiber, thus leading to a skin-core variation well suited for the bonding process. This topic is discussed in the next subsection.

If the draw-down ratio is too high, the molten filament will break due to flow instabilities. At slightly lower draw-down ratios, the fibers produced may have a large content of imperfections, a inhomogenous structure (along the fiber), and/or large diameter fluctuations. This would perhaps again weaken the fibers, as we believe is the case with the fibers A5 and A6. There must, therefore, exist an upper optimal value for the draw-down ratio, which depends on the other processing parameters.

Skin-Core Structures

The radial variation of the fiber structure/morphology may be optimized in order to enhance thermal bonding, and to minimize the reduction of fiber strength due to heat and stress in the bonding process. Some aspects of this skin-core differentiation are summarized below.

Maximum birefringence, i.e., molecular orientation, at the surface is a characteristic of fibers spun at high draw-down ratios, i.e., with high tensile stresses.[43–46] Fibers spun at lower speeds, and subsequently drawn, have no radial variation or maximum orientation in the core. These observations can be explained as follows: in the spinning stage, radial temperature profiles lead to a higher axial stress at the surface, which is cooled faster than the core and therefore has a higher viscosity. Parabolic radial birefringence distributions have been observed in several spinning stage studies involving amorphous polymers. For semicrystalline polymers the profiles can be more complex.[47] Subsequent drawing at elevated temperatures can alter the profile so that the core obtains the highest orientation. This can be explained by reversing the argument given for the spinning stage. In the spinning of polypropylene, the solidification is usually dominated by deformation-induced crystallization. However, fibers with highest orientation in the skin layer do not necessarily have the highest degree of crystallinity in this layer. The size/perfection of the crystallites is probably smaller/lower in the skin layer, due to the rapid cooling and high tension.

According to Marcher,[3] the bondability index of

a fabric made of fibers spun in a conventional process is typically 60% higher than that of a fabric made of fibers spun in a compact process. In both cases the fibers are drawn after spinning, at almost identical conditions. These differences can partly be related to different skin-core structures. According to Marcher, the conventional process permits a "controlled degradation" of the surface, which increases the bondability of the fibers. From molecular weight measurements before and after spinning, it is clear that the polymer is degraded during melt spinning. The surface layer of the fiber is in contact with air and experiences the highest stress. Hence, the surface layer should experience the highest degradation.

So, which skin structures are optimal for thermal bonding? Some factors that usually lead to a decrease in melting temperature are reductions in crystal size, crystal order, and molecular weight. The effect of molecular orientation (in crystalline and amorphous phases) is not so clear.[36] The bulk melting temperature is often reported to increase with increasing orientation, but the results from thermal analysis of oriented polymers depend on how the samples are prepared.

The only relevant characterizations of skin-core profiles, found in the literature on melt spun fibers, are the birefringence measurements cited above. No direct information has been reported about important topics such as order, size, and orientation of crystalline and amorphous phases. Several methods may supply information of this kind. Tshmel et al.[48] performed IR Attenduated Total Reflection (ATR) measurements on ultradrawn polyethylene fibers. An "integrated" optical element was molded around a sample consisting of parallel fibers. Effective penetration depths in the range 0.6–5.0 μm were achived by varying the angle of incidence, the polarization, and the wave number. Secondary Ion Mass Spectrometry (SIMS) is another candidate for studying the surface layer.

The skin-core differentiation, as well as the morphology of the different layers, can be modified by adding certain nucleating agents and antioxidants.[30] For PP cast film, for instance, it is shown that certain combinations of processing conditions and nucleating agents are able to reverse the skin-core structure.[49] A research report from Himont stated that they had modified polypropylene by the addition of the dianhydride of benzophenone tetracarboxylic acid or alkyl derivatives of this, to produce better bonding properties.[13,30] In the mid-eighties, Moplefan, in cooperation with Himont, developed a new generation of PP fibers with extraordinary good bonding properties.[5,7,8] According to Moplefan, this was due to the skin-core structure, but no details were given about additives and processing parameters. Compared to other fibers optimized for thermal bonding, these Moplefan fibers have higher strength and lower elongation at maximum load.[8] WAXS analyses of a selection of commercial fibers used in thermally bonded nonwovens[50] revealed that only the Moplefan fibers lacked bimodal orientation, which indicates a higher draw ratio. Nonwovens made of these Moplefan fibers have higher strength and higher elongation at maximum load. Moplefan claim that their fibers give high bond strength independently of the strength of the fiber, due to the intrinsic structure. However, for conventional fibers, as in this study, the bond properties are sensitive to the strength of the fiber, which is mainly determined by the draw ratio.

One of the most common bicomponent fibers used in thermally bonded nonwovens is based on the skin-core principle, with PP as core and PE (with a lower melting point) as skin.

Extrusion Temperature

With the truncated design in Table I, only the pairs NA1/NA3 and NA2/NA4 (with extrusion temperature 260/240°C) reveal some information about the effect of extrusion temperature. As mentioned above, the MD strengths are roughly the same at these two extrusion temperatures. The bondability index seems to increase with increasing extrusion temperature, and the anisotropy index seems to decrease. These two trends are usually connected, and a higher bondability index for the highest extrusion temperature may be due to a higher degree of degradation at the fiber surface, which may facilitate bonding as mentioned in the preceding subsection.

Macroscopic Fracture Mechanisms

There are three possible mechanisms for the fracture of nonwoven fabrics in tensile deformation: (1) fracture between bonds, (2) fracture at the bond perimeter, and (3) detoriation of the bonds, followed by fiber fracture.

Judging from the load–elongation curves, there seems to be some differences in the fracture mechanisms. The MD load decreases in one or several steps before the ultimate fracture. The fracture seems to be more abrupt for the strongest nonwovens, i.e., the distribution of "link" strengths is narrower. However, fibers in strong nonwovens do not have narrower distributions of elongation and load at break. Hence, the difference in fracture mechanisms must be due to the bonding. Load-elongation

curves for NA5 (Fig. 3) and NA9 (Fig. 4) illustrate the two mechanisms. The load of the former nonwoven decreases in a large number of steps on a long elongation interval. In contrast to this, all the parallels of the latter nonwoven fracture abruptly. Strong nonwovens generally have the highest elongation at maximum load (or break) as well. This is true for both MD and CD results (see Table III).

SEM studies indicate that the strong nonwovens generally have a higher degree of welding (interfilament cocrystallization) at the bonding points. Single fibers can hardly be distinguished. Also, the degree of welding decreases more gradually at the perimeter of the bonding point. For the weak nonwovens, some of the fibers seem to be damaged at the perimeter.

Fabrics that had been stretched to break were also examined. Bonding points near the fracture line were studied to gain some information about the fracture mechanisms. Weak nonwovens seem to fracture in two stages: (1) disintegration of bonding points into single fibers, and (2) deformation and fracture of fibers. For these nonwovens, the fibers usually fracture at segments that have been inside a bonding area. Fibers in strong nonwovens, on the other hand, preferably break at the bonding point perimeter. This agrees with the abrupt behavior seen for the load–elongation curves (see Fig. 4).

In contrast to this, some of the literature on fracture mechanisms in nonwovens indicate that the "optimum" fracture mechanism is one that is dominated by bonding point disintegration. Warner[18] studied the deformation and fracture of nonwovens. Microscopy (optical and SEM) and tensile deformation were conducted simultaneously. Warner observed that the sample buckled in the cross-direction due to Poisson effects. The buckling was inhomogenous because of the rigidity of the bond points. Holes were formed within the bond spots. The holes probably originated as a result of the complex stresses set up by the wide distribution of forces on each of the fibers in the fabric. Fracture occurred in a number of different ways, depending on the local characteristics of the fabric. Some bond points disintegrated, and sometimes the fracture was strictly between bonds. Fracture of about 60% of the fibers occurred at the bond perimeter. According to Warner,[26] the material at the bond perimeter is often weak and/or brittle due to its thermomechanical history. Hence, he claimed that the strength of most calender-bonded fabrics is limited by the mechanical properties of the material at the bond perimeter. Olivieri[6] compared the fracture mechanisms of nonwovens made of "conventional" fibers and Moplefan TG fibers. In the former case, the bond spot broke up as a whole structure, into a few parts. In the latter case, the fibers involved in the bond spot separated individually, contributing to the tensile resistance of the bond spot with all the fiber-to-fiber bonds. The fibers that separated under tension showed traces of breakage of the single interfiber bonds. According to Landoll et al.,[8] SEM studies show that different fracture mechanisms are active below and above the optimum bonding temperature. Below this temperature, the bond spots disintegrate. Above the optimum bonding temperature the fibers break at the bond perimeter. At the optimum bonding temperature both mechanisms are active, but bond disintegration is dominant.

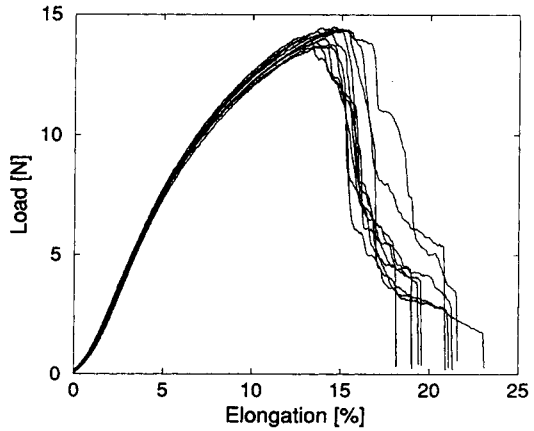

Figure 3 MD load–elongation curves (10 parallels) for NA5 bonded at 152°C.

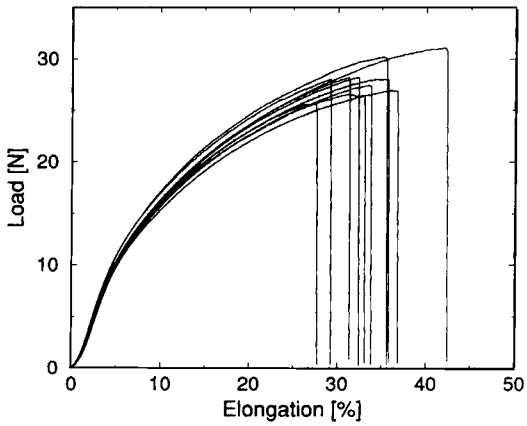

Figure 4 MD load–elongation curves (10 parallels) for NA9 bonded at 152°C.

SUMMARY AND CONCLUSION

In the processing regime considered in this study, the properties of the fibers can be summarized as

follows: α-crystalline structure with various degrees of bimodal orientation was obtained for all combinations of material and processing parameters. The degree of orientation increases with increasing draw ratio and decreasing M_w/M_n, and it increases with increasing draw-down ratio for narrow MWDs. The tensile strength increases with increasing draw ratio (via increased orientation) and decreasing M_w/M_n (mainly due to different deformation mechanisms for broad and narrow MWDs), and it seems to have a maximum as a function of draw-down ratio. The onset of melting increases with increasing M_w/M_n, decreasing draw ratio and decreasing extrusion temperature.

The parameter that has the greatest influence on the fabric strength is the calender roll temperature. The fabric strength increases with increasing roll temperature. The tensile properties of the nonwovens are also influenced by the MWD and the processing conditions of the fibers. The relative effects of these fiber parameters increase with increasing roll temperature. There is no direct relation between the melting point of constituent fibers and the strength of nonwovens.

The fabric strength increases with increasing M_w/M_n, decreasing draw ratio and increasing extrusion temperature (in these three cases the fiber strength generally follows the opposite trend). Furthermore, the fabric strength (as well as the fiber strength) has a maximum as a function of draw-down ratio. Our tentative explanations for these effects are as follows: the presence of a high molecular weight tail and high draw-down ratios seem to facilitate structures that are well preserved in the bonding process. High draw-down ratios and extrusion temperature may lead to degradation of the fiber surface, and, hence, a skin-core structure well suited for the bonding process. However, too high draw-down ratios may induce defects and diameter variations that reduce the strength of both fibers and fabrics. High draw ratios lead to high molecular orientation, which is detrimental for the cocrystallization. Fibers with high draw ratios may also be more prone to defects induced by the heat and stress during the bonding process.

Hence, the tensile properties of the nonwovens seem to be mainly governed by the bonding properties, not the strength, of the constituent fibers. In order to optimize the nonwoven strength, the fibers should have a skin–core structure with differential melting behavior. The surface layer should have a high ability for cocrystallization, not just a lower melting point. Furthermore, the structure should not be prone to defects caused by heat and stress.

From the load–elongation curves it can be seen that strong nonwovens fracture more abruptly, i.e., the load decreases more steeply after having reached its maximum value. SEM studies indicate that the strong nonwovens fracture via fiber breakage at bonding point perimeters, while the weak nonwovens fracture by bonding point disintegration, followed by fiber breakage at segments previously inside the bonding area. Judging from the literature, different fracture mechanisms may be the optimum, depending on the bonding temperature, the skin–core structure, and the design of bonding points.

This article is based on results from the 'Expomat Fiber Project,' supported by Borealis and the Research Council of Norway. The authors would like to thank E. Glawion (Rieter-Automatik, Germany), O. T. Turunen, and O. Tuominen (both at Borealis, Finland) for technical assistance.

REFERENCES

1. A. Drehlich and R. L. Smorada, in *Encyclopedia of Polymer Science and Engineering*, 2nd ed., Vol. 10, Wiley, New York, 1989, p. 204.
2. C. J. Shimalla and J. C. Whitwell, *Text. Res. J.*, **46**, 405 (1976).
3. B. Marcher, in *Proceedings from the INDEX 93 Congress*, Geneva, Switzerland, 1993.
4. V. Rossi, *Vliesstoff Nonwoven Int.*, **5**(3), 86 (1990).
5. P. Olivieri, *Nonwovens Rep. Int.*, August 1990, p. 30.
6. N. N., *Nonwovens Rep. Int.*, March 1988, p. 10.
7. P. Olivieri, *Nonwovens Rep. Int.*, March 1988, p. 15.
8. P. Olivieri, M. Branchesi, and T. Ricupero, in *Proceedings from the 4th Int. Conf. on Polypropylene Fibers and Textiles*, Nottingham, UK, 1987.
9. J. Krag, in *Proceedings from the 4th Int. Conf. on Polypropylene Fibers and Textiles*, Nottingham, UK, 1987.
10. L. M. Landoll and B. J. Hostetter, in *Proceedings from the 4th Int. Conf. Polypropylene Fibers and Textiles*, Nottingham, UK, 1987.
11. K. L. Floyd, *Nonwovens Yearbook*, 1986, p. 25.
12. K. Y. Wei, T. L. Vigo, and B. C. Goswami, *J. Appl. Polym. Sci.*, **30**, 1523 (1985).
13. N. N., *Nonwovens Rep. Int.*, January 1985, p. 8.
14. D. H. Müller and S. Barnhardt, *Nonwovens Rep. Int.*, March 1986, p. 19.
15. D. H. Müller, *Vliesstoff Nonwoven Int.*, **4**(1), 22 (1989).
16. C. K. Deakyne, L. Rebenfeld, and J. C. Whitwell, *Text. Res. J.*, **47**, 491 (1977).
17. C. J. Shimalla and J. C. Whitwell, *Text. Res. J.*, **46**, 513 (1976).
18. V. Röhring and W. Pazolt, in *Proceedings from the INDEX 93 Congress*, Geneva, Switzerland, 1993.

19. S. Klöcker, in *Proceedings from the INDEX 93 Congress,* Geneva, Switzerland, 1993.
20. K. E. Duckett and S. Kanagaraj, *INDA J. Nonwovens Res.*, **4,** 16 (1992).
21. S. B. Warner, *Text. Res. J.*, **59,** 151 (1989).
22. O. Jirsak and D. Lukas, in *Proceedings from the INDEX 93 Congress,* Geneva, Switzerland, 1993.
23. T. H. Grindstaff and S. M. Hansen, *Text. Res. J.*, **56,** 383 (1986).
24. P. N. Britton, A, J. Sampson, and W. E. Gettys, *Text. Res. J.*, **54,** 425 (1984).
25. P. N. Britton, A, J. Sampson, and W. E. Gettys, *Text. Res. J.*, **54,** 1 (1984).
26. P. N. Britton, A. J. Sampson, C. F. Elliot, H. W. Graben, and W. E. Gettys, *Text. Res. J.*, **53,** 363 (1983).
27. S. K. Mukhopadhyay, *J. Text. Inst.*, **83,** 573 (1992).
28. S. K. Mukhopadhyay and P. W. Foster, *J. Text. Inst.*, **81,** 135 (1990).
29. S. K. Mukhopadhyay, J. W. S. Hearle, and P. W. Foster, *J. Text. Inst.*, **79,** 235 (1988).
30. S. K. Mukhopadhyay and P. W. Foster, in *Proceedings from the 4th Int. Conf. on Polypropylene Fibers and Textiles,* Nottingham, UK, 1987.
31. W. A. Fraser and J. C. Whitwell, *Text. Res. J.*, **42,** 1003 (1971).
32. S. B. Warner, in *Proceedings from ANTEC '88,* Atlanta, GA, 1988.
33. E. Andreassen and O. J. Myhre. *J. Appl. Polym. Sci.*, **50,** 1715 (1993).
34. E. Andreassen, O. J. Myhre, E. L. Hinrichsen, and K. Grøstad, *J. Appl. Polym. Sci.*, **52,** 1505 (1994).
35. E. Andreassen, E. L. Hinrichsen, K. Grøstad, O. J. Myhre, and M. D. Braathen, *Polymer,* **36,** 1189 (1995).
36. E. Andreassen, K. Grøstad, O. J. Myhre, M. D. Braathen, E. L. Hinrichsen, A. M. V. Syre, and T. B. Løvgren, *J. Appl. Polym. Sci.*, **57,** 1075 (1995).
37. E. Andreassen, O. J. Myhre, F. Oldervoll, E. L. Hinrichsen, K. Grøstad, and M. D. Braathen, *J. Appl. Polym. Sci.*, to appear.
38. M. Ahmed, *Polypropylene Fibers—Science and Technology,* Elsevier, Amsterdam, 1982.
39. F.-M. Lu and J. E. Spruiell, *J. Appl. Polym. Sci.*, **34,** 1521 (1987).
40. R. A. Gill and C. Benjamin, *Plastics Rubbers Proc.*, **5,** 25 (1980).
41. H. J. Yoo, *Polym. Eng. Sci.*, **27,** 192 (1987).
42. O. Hånde, to appear.
43. H. J. Kang and J. L. White, *Int. Polym. Proc.*, **1,** 12 (1986).
44. G. Vassilatos, B. H. Knox, and H. R. E. Frankfort, in High-Speed Fiber Spinning, A. Ziabicki and H. Kawai, Eds., Wiley, New York, 1985.
45. G. Perez, in *High-Speed Fiber Spinning*, A. Ziabicki and H. Kawai, Eds., Wiley, New York, 1985.
46. A. Ziabicki, in *High-Speed Fiber Spinning*, A. Ziabicki and H. Kawai, Eds., Wiley, New York, 1985.
47. P. Y.-F. Fung, E. Orlando, and S. H. Carr, *Polym. Eng. Sci.*, **13,** 295 (1973).
48. A. Tshmel, I. A. Gorshkova, and V. M. Zolotarev, *J. Macromol. Sci.-Phys.*, **B32,** 1 (1993).
49. M. Akay, in *Proceedings from the 4th Int. Conf. on Polypropylene Fibers and Textiles,* Nottingham, UK, 1987.
50. E. Andreassen and O. J. Myhre, unpublished results.

Received June 10, 1995
Accepted June 25, 1995